www.crt-journal.org

Crystal Research and Technology

Journal of Experimental and Industrial Crystallography
Zeitschrift für experimentelle und technische Kristallographie

WILEY-VCH

Cryst. Res. Technol. **45**, No. 7, 685 – 691 (2010) / **DOI** 10.1002/crat.201000163

Thermal transformations of the mineral component of composite biomaterials based on chitosan and apatite

S. N. Danilchenko*[1], O. V. Kalinkevich[1], V. N. Kuznetsov[1], A. N. Kalinkevich[1], T. G. Kalinichenko[1], I. N. Poddubny[1], V. V. Starikov[2], A. M. Sklyar[3], and L. F. Sukhodub[1]

[1] Institute for applied physics, Sumy, Ukraine
[2] National technical university "Kharkov polytechnic institute", Kharkov, Ukraine
[3] Sumy state pedagogical university, Sumy, Ukraine

Received 12 March 2010, revised 31 March 2010, accepted 7 April 2010
Published online 23 April 2010

Key words apatite, chitosan, composite biomaterials, annealing, X-ray diffraction.

Composite biomaterials based on chitosan and calcium apatite with different chitosan/apatite ratio were prepared by chemical synthesis of apatite in chitosan solution using one-step co-precipitation method. Initial and annealed samples were characterized by X-ray diffraction, FTIR spectroscopy and scanning electron microscopy coupled to energy-dispersive electron X-ray spectroscopy. The data obtained suggest that the formation of the calcium-phosphate mineral in chitosan solution is substantially modulated by the chemical interaction of the components; apparently, a part of calcium is captured by chitosan and does not participate in the formation of the main mineral phase. The apatite in the composite is calcium-deficient, carbonate-substituted and is composed of dispersed nano-sized crystallites, i.e. has properties that closely resemble those of bone mineral. Varying synthesis, drying and lyophilization conditions, the composite materials can be produced with the desirable chitosan/apatite ratio, both in the dense and porous form. The structural analysis of composite samples after annealing at certain temperatures is examined as an approach to elucidate the mechanism of co-precipitation by one-step method.

1 Introduction

The current interest to the biomaterials based on chitosan and calcium apatite [1-6] is caused by their high biocompatibility, good mechanical characteristics, relatively low price and simplicity of preparation and characterization. Structurally these materials resemble the natural bone tissue, in which the fibrillar protein collagen serves as an elastic matrix, while the nanocrystals of biogenic apatite reinforce the bone strength [7]. In the chitosan-apatite composites the high-molecular chains of natural polysaccharide chitosan function as an elastic matrix, while the synthetic apatite is a reinforcing component. Chitosan is the simplest derivative of chitin produced by its deacetylation. Chitin is an abundant natural polysaccharide, it is the base of the skeletal system of *Crustacea*, cuticule of insects, cell walls of fungi and some bacteria. Hydroxyapatite (HA, $Ca_{10}(PO_4)_6(OH)_2$) can, with some approximation, be regarded as a crystallochemical analogue of mineral part of animal and human skeletons. It has been used for a long time as a basic component of a wide range of synthetic materials in orthopaedy and dentistry [8].

Recently the interest in chitosan-apatite composite biomaterials has increased significantly, evidenced by the growth of related scientific papers number. Different preparation methods of such materials production have been developed. Most of them involve two major stages: first, the synthesis of the organic polymeric scaffolds of pure or chemically treated and modified chitosan; and second, mineralization of the scaffold either in the simulated body fluid (the biomimetic way) or in saturated matrix solutions [2,5,9]. An inverse approach has also been described – the pre-formation of a porous hydroxyapatite scaffold followed by its impregnation with chitosan [10]. Yamaguchi et al. [1] have described a one-step scheme of chitosan-hydroxyapatite synthesis, in which the composite was co-precipitated by dropping chitosan solution containing phosphoric acid into a calcium hydroxide suspension. Rusu et al. have developed a co-precipitation approach using it to

* Corresponding author: e-mail: danil50@hotbox.ru

obtain different types of chitosan-hydroxyapatite composites with different ratios between the components [4]. A further improvement of this approach was pursued by Chesnutt et al., who developed microsphere-based chitosan-nanocrystalline calcium phosphate composite scaffolds [6]. The composite materials prepared by one-step co-precipitation method consist of nano-sized hydroxyapatite with morphology and structural features close to those of biological apatites. In addition, this preparation technique provides the homogeneous chitosan-apatite composite with the developed contact interface area between the mineral phase and the organic matrix.

Among the large number of works dealing with the examination of biocomposites based of apatite and chitin/chitosan, only a small part describes the thermal transformations in the calcium phosphate component of these materials [e.g. 9,11]. Such studies are necessary because the synthesized apatite in the composite is nanocrystalline, i.e. its X-ray diffraction lines are diffused and overlapped due to small size of crystallites and lattice distortions. Therefore, the estimation of the structural characteristics is complicated and ambiguous. To examine the phase stability and to disclose the imperfection of the nanocrystalline apatite it is necessary to perform the temperature tests, particularly annealing up to certain characteristic temperatures and the structural studies of the formed products. Comparing the test results of the materials with different chitosan/apatite ratio, as well as of synthetic and biogenic apatite, it is possible to study the interaction of organic and mineral components in the composite [12,13]. Besides, the information about the weight loss of the composites after annealing allows the estimation of bound water content and mineral-to-organic ratio [1,9]. Here we report the results of a structural examination of the calcium apatite synthesized in chitosan solution by one-step co-precipitation method and subjected to heat treatments at increased temperatures.

2 Experimental

Sample preparation To obtain chitosan-apatite composite (ChAp) the 1 M solution of $CaCl_2$ and 1 M solution of NaH_2PO_4 were used. The co-precipitation (for ChAp with 50/50 wt% ratio, as an example) was performed as follows: 20 ml of $CaCl_2$ solution and 12 ml of NaH_2PO_4 solution (molar ratio Ca/P=1.67) were added to 1000 ml of 0.2% solution of low-molecular chitosan from krill (Aldrich) in 1% acetic acid. Then pH of the solution was brought to 11 using 1.25 M NaOH. The obtained suspension was aged for 24 h to form a hydrogel. The hydrogel then have been rinsed with distilled water till the neutral reaction of flushing water. After drying the hydrogel at room temperature, the solid ceramic-like composite material was formed. Varying volumes of salt solutions we obtained the samples with the following chitosan/apatite ratio: 15/85, 30/70, 50/50, 80/20 (Table 1). The porous materials were prepared by lyophilization of the wet gel in the home made glass vacuum system with liquid nitrogen. Initial samples were annealed in the electric furnace in the air under the temperatures of 130 °C, 400 °C, 700 °C, 900 °C and 1100 °C exposing to each fixed temperature during 45 min. For each case the temperature raise was relatively slow (about 0.05 Ks^{-1}) to provide quasi-stationary conditions.

Materials characterization The amount of water and chitosan/apatite ratio in the composites were estimated by weighing the samples before and after annealing at the temperatures of 130 °C and 900 °C, assuming that the weight loss at 130 °C corresponds to the removal of the water fraction only, while at 900 °C only to the polysaccharide fraction [1].

X-ray diffraction (XRD) analysis was carried out on DRON4-07 diffractometer (“Burevestnik”, Russia) connected to computer-aided system for the experiment control and data processing. The Ni-filtered CuKα radiation (wavelength 0.154 nm) with a conventional Bragg-Brentano ϑ-2ϑ geometry was used (2ϑ is the Bragg’s angle) [14]. The current and the voltage of the X-ray tube were 20 mA and 30 kV respectively. The samples were measured in the continuous registration mode (at the speed of 1.0 °/min) within the 2ϑ-angle range from 10° to 60°. All experimental data processing procedures were carried out with the use of the program package DIFWIN-1 (“Etalon PTC” Ltd, Russia). The separation of overlapping diffraction lines was done with the freeware program New_Profile3.4 (http://remaxsoft.ru/).

Scanning electron microscopy (SEM) with X-ray emission spectroscopy was performed using the REMMA-102 device (SELMI, Ukraine). The energy dispersive X-ray (EDX) detector was used. The analytical signal of characteristic X-ray emission was integrated by scanning the 50×50 μm^2 area of the sample surface. To avoid the surface charge accumulation in the electron-probe experiment, the samples were covered with a thin (30-50 nm) layer of silver in a VUP-5M vacuum device (SELMI, Ukraine).

Infrared spectra were recorded by the Spectrum-One FTIR spectrometer (Perkin Elmer). Before the measurements the powdered samples were mixed with the KBr powder (2.5-3.0 mg of a sample per 300 mg of

KBr) and pressed to the tablets. The Vickers hardness of the initial samples was measured by the standard method using the special light microscope PMT-3 (LOMO, Russia).

3 Results and discussion

As it can be seen from table 1, the chitosa/apatite ratio determined by weighing the samples after annealing at 900 °C is in reasonable agreement with the values specified at the synthesis. Therefore, the assumption that the polysaccharide component is completely removed by heat treatment from the ChAp samples is correct, as well as that the present conditions of synthesis allow obtaining of the desired chitosan/apatite ratio. After decomposition and combustion of the organic component the samples should be considered as an inorganic material.

Table 1 Synthesis conditions and thermogravimetric characteristics of ChAp composites.

Code of ChAp sample (desired weight ratio)	Preparation conditions				Data of thermogravimetric analysis			
	Chitosan solution		Ca and P salts solutions		Percentage of the components			Chitosan/ apatite weight ratio
	C, wt %	V, ml	$CaCl_2$ 1M, V, ml	NaH_2PO_4 1M, V, ml	H_2O, wt %	chitosan, wt %	apatite, wt %	
ChAp 15/85	0.2	1000	113.3	68.0	9.0	14.9	76.1	16.4/83.6
ChAp 30/70	0.2	1000	46.6	28.0	11.4	25.4	63.2	28.7/71.3
ChAp 50/50	0.2	1000	20.0	12.0	5.3	48.8	45.9	51.5/48.5
ChAp 80/20	0.2	1000	5.0	3.0	8.9	73.0	18.1	80.1/19.9

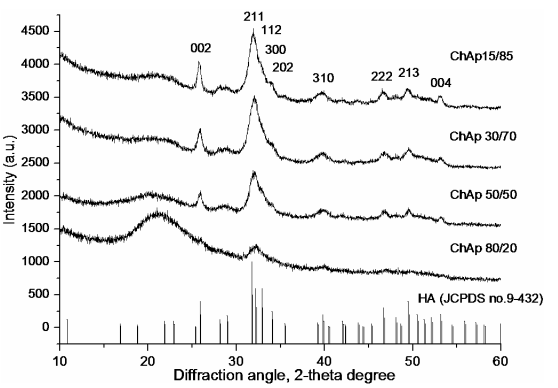

Fig. 1 X-ray diffraction patterns of ChAp samples with different initial component ratios; the lines marked with Miller indices belong to HA. At the bottom there is the theoretical pattern of HA according to JCPDS.

The X-ray diffraction patterns of the initial composite materials indicate the presence of poorly crystalline apatite, its crystallinity decreasing with the increase of chitosan component content (Fig. 1). The main diffraction lines, marked in the diffraction pattern of the ChAp 15/85 sample by Miller's indices (JCPDS No. 9-432), agree well with the tabular data. From the broadening of diffraction lines, which is inversely proportional to the crystallite size, it follows that the more chitosan a composite contains, the less is the average size of apatite crystallites. Qualitative estimation of main diffraction lines' profile width shows that for the ChAp 30/70 the crystallite (crystal domain) size of apatite in the composite is comparable with the size of bone tissue bioapatite crystallites (~20 nm) [13,15].

It should be noted that X-ray diffraction data of the initial chitosan-apatite samples are not well informative, and even at the maximal content of apatite (sample ChAp 15/85) do not allow quantitative characterization of the mineral, e.g. it is impossible to determine the size of the apatite unit cell with sufficient accuracy or to detect the traces of other phases.

According to the SEM data, the particles of the synthesized composite materials have the solid surface: smooth (Fig. 2a), or laminated and slightly perforated (Fig. 2b). No visible signs of the separation or foliation of the material into mineral and organic parts were observed. The use of freeze-drying immediately after rinsing and partial ageing of the samples allowed significant modification of the material microstructure, e.g. pore formation (Fig. 2c and 2d). The characteristics of pores (size and uniformity, shape and extent), were found to be significantly dependent both on the lyophilization conditions (temperature, duration, initial humidity of the material) and on the initial chitosan/apatite ratio. Thus, before the processes of ageing and drying are completed, the "raw" chitosan-apatite composite is able to form microporous structure under

lyophilization. So, selecting the proper component ratio and lyophilization conditions, one can achieve the desired porosity of the composite biomaterial.

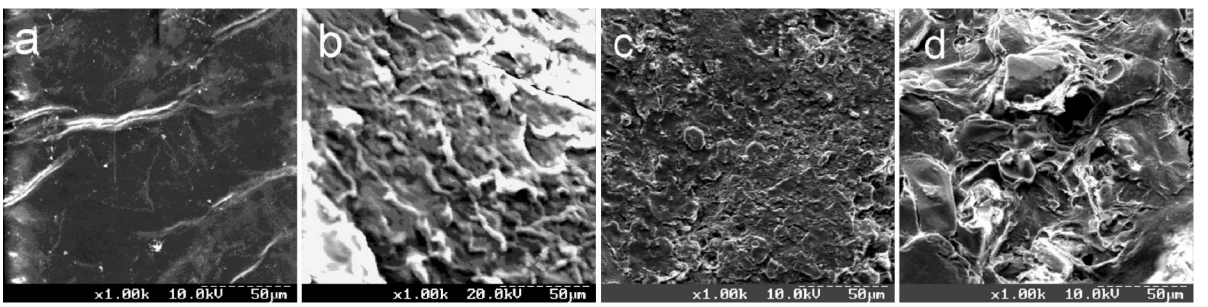

Fig. 2 SEM micrographs of the surface of the initial ChAp samples with 50/50 chitosan/apatite ratio (a and b); and of the samples after freeze-drying with chitosan/apatite ratio 15/85 (c) and 50/50 (d).

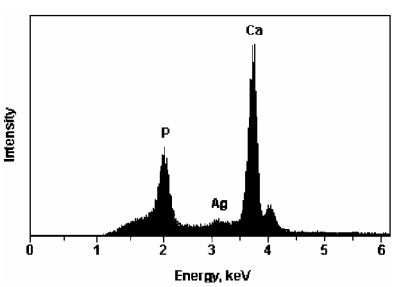

Fig. 3 EDX spectrum of the ChAp 50/50 composite. Ag signal is from the deposited thin conducting Ag film.

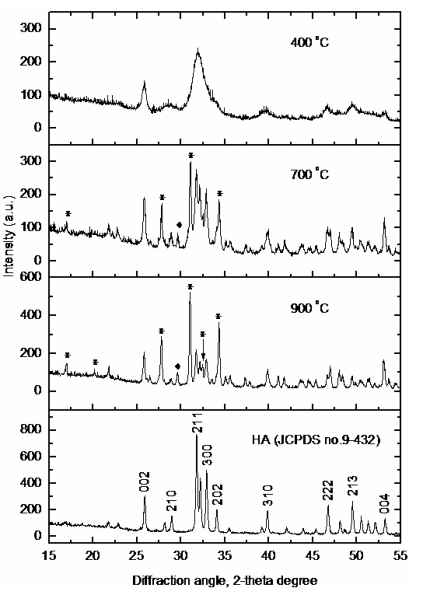

Fig. 4 X-ray diffraction patterns of ChAp 30/70 samples temperature row (the asterisks mark the major peaks of $Ca_3(PO_4)_2$, the diamonds mark the strongest diffraction lines of $CaCO_3$); at the bottom there is the pattern of the pure HA.

In the characteristic X-ray emission (EDX) spectra of the initial ChAp samples only the intense peaks of Ca and P were observed, while peaks from Na and Cl were not detected (Fig. 3). This indicates that sodium and chlorine from the mother solutions did not pass into the precipitate, and so the obtained synthetic apatite did not have the substitutions in cation (Na→Ca) and anion (Cl→OH) sublattices. The quantitative estimation of Ca/P ratio shows the excess content of Ca compared with the value corresponding to the stoichiometric hydroxyapatite (1.67, atomic ratio). With the increase of chitosan/apatite ratio in the composites, the Ca/P ratio also increases: for the samples ChAp 15/85, ChAp 50/50 and ChAp 80/20 it amounts to 1.78, 1.93 and 2.15, respectively.

The initial samples of non-porous ChAp composites have good strength characteristics. The Vickers hardness is 0.22 GPa, 0.15 GPa, 0.12 GPa and 0.14 GPa for the ChAp 15/85, ChAp 30/70, ChAp 50/50 and ChAp 80/20, respectively. These data indicate the decrease of material strength with the increase of chitosan percentage and are in reasonable agreement with the value of 0.396 GPa recently reported for the cortical bone [16]. The porous composite materials are much less hard than the solid ones; their measured hardness values were too much spread to be conclusive; it was difficult to measure the dent size because of the complicated profile of the sample surface.

The choice of temperatures at which the initial composite materials have been annealed was caused by the facts that in the biogenic and synthetic apatite after 700 °C the significant increase of crystallite size is observed [13]; after annealing at 900 and 1100 °C the emergence and development of other crystalline phases is possible, which is caused by structural and concentrational imperfections of initial apatite [8,17]. Therefore, comparing the phase composition and substructure characteristics in the temperature series of samples with different chitosan/apatite ratios it is possible to make certain conclusions about the formation of the initial nanocrystalline apatite in the presence of chitosan.

The X-ray phase analysis has shown that the formation of the β-tricalcium phosphate (β-TCP, $Ca_3(PO_4)_2$, JCPDS No. 9-169) phase in the annealed samples takes place, together with the recrystallization processes in the apatite phase (Fig. 4), which indicates the Ca deficiency in the initial nanocrystalline apatite [18]. The increase of chitosan content in the composites leads to the increase of the amount of β-TCP forming under annealing. In addition, with the increase of chitosan content, the crystallinity of apatite in the samples annealed at 900 °C decreases significantly. Nevertheless, the structural features of apatite formed under annealing seem to match satisfactorily with those of standard HA.

The results of XRD quantitative phase analysis (according to the procedure [18]) and evaluation of crystallite sizes for HA and β-TCP phases from the broadening of some appropriate lines (according to Scherrer [14,15]) are summarized in the table 2. It should be noted that crystallite sizes determined from Scherrer's equation are suitable only for rough estimation due to the ignoring of lattice strain contribution in the diffraction line broadening [15]. Moreover, all selected lines are overlapped with neighboring ones and therefore need to be separated. Especially it applies to the (002) lines of HA for which the accuracy of crystallite size determination is worse. Nevertheless, these evaluation data are quite suitable for comparison with other works.

Table 2 Calculated XRD data of HA/TCP phase ratio (assuming two phase system) and crystallite (crystal domain) size of HA and β-TCP phases.

Sample code	Annealing temperature, ºC	Phase ratio HA/β-TCP, wt %	Average crystallite size of HA and β-TCP phases, nm			
			HA along [002]	HA along [300]	HA along [211]	β-TCP along [0210]
ChAp 15/85	400	β-TCP not detected	34	no data	no data	no data
	700	70.6/29.4	34	26	27	29
	900	41.2/58.8	55	48	45	52
	1100	46.9/53.1	51	40	55	49
ChAp 30/70	400	β-TCP not detected	16	no data	no data	no data
	700	46.6/53.44	36	34	18	39
	900	23.6/76.4	39	30	30	41

Comparing the values of crystallite size for HA phase of ChAp composite annealed at 900 °C with the similar values of annealed pure HA and bone samples [13], we can note that crystallites in the composite grow under annealing more slowly and reach much smaller sizes than the crystallites of synthetic and biogenic apatites. Probably, the slower temperature growth of crystallites in composites is caused by the dispersed and homogeneous distribution of randomly oriented calcium phosphate nanocrystals in chitosan matrix, which complicates and slows down the sintering and recrystallization processes in crystallites.

It should be noted that the more detailed analysis of the XRD pattern of the samples annealed at 700 °C and higher reveals the presence of small amounts (3-5 %) of the calcite phase ($CaCO_3$, JCPDS No. 70-95). No explicit regularities in the changes of $CaCO_3$ content depending on the chitosan/apatite ratio or the annealing temperature were found for the present time. As it is seen from the XRD profile comparison (Fig. 1 and Fig. 4), under annealing below 400 °C no noticeable changes in the structure of nanocrystalline apatite take place. The growth of apatite crystallites and emergence of β-TCP and $CaCO_3$ phases appear pronouncedly in all samples starting from the annealing temperature of 700 °C.

The formation of β-TCP and HA phases in the annealed materials is the evidence that the initial nanocrystalline apatite was Ca deficient. The emergence of $CaCO_3$ phase partially or totally compensates this deficiency in the whole volume of a sample; this is in agreement with the data of EDX indicating the excess content of Ca in ChAp samples as compared with the pure HA. This excessive Ca is supposed to be non-apatite one. It contributes to the total content of Ca measured by EDX, while the forming apatite crystals are Ca-deficient. Apparently, the non-apatite Ca under annealing gets into the $CaCO_3$ phase. These experimental data

suggest the partial localization of calcium out of the volume of mineral part of initial composites. Probably, a part of initial calcium is entrapped by the chitosan molecules, so the forming nanocrystalline apatite grows as calcium-deficient and, when thermally decomposed, forms the biphasic system HA + β-TCP. The $CaCO_3$ phase is probably formed as a result of polysaccharide pyrolysis with the participation of Ca previously (at the co-precipitation stage) entrapped by chitosan.

The IR absorption spectra for the series of ChAp 50/50 samples (as an example) are shown in figure 5. The bands in the region of 1092–1090 cm^{-1} and 1049–1047 cm^{-1} are connected with degenerate antisymmetric ν_3 P-O valence oscillations of the phosphate groups. The band at 962 cm^{-1} corresponds to the nondegenerate ν_1 P-O symmetric valence oscillations, while the doublet at 602–573 cm^{-1} can be ascribed to ν_4 O-P-O deformation vibrations [19,20]. The intensity of phosphate bands in the IR spectrum of the initial composite is relatively low. This could be due to the very small size of apatite crystals, so that the hydration layer on their surface hampers the oscillations of phosphate ions.

It should be kept in mind that according to XRD data, annealing up to 400 °C did not initiate any visible structural changes in the primary apatite, while above 700 °C the heating-induced variations emerged in the multi-phase system. Therefore, the IR spectrum shown in figure 5b corresponds to the initial mineral after the loss of loose water and combustion of the organic component; the spectra in figure 5c, 5d correspond to the inorganic material containing HA, β-TCP and $CaCO_3$ phases. This fact can explain some broadening, distortion and displacement of the IR bands from their standard positions.

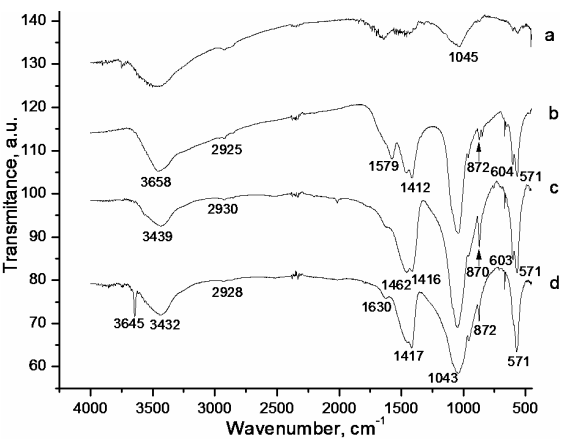

Fig. 5 IR spectra of ChAp 50/50 samples temperature series (a, b, c, d correspond to the initial sample and annealed ones at 400, 700, 900 ºC, respectively).

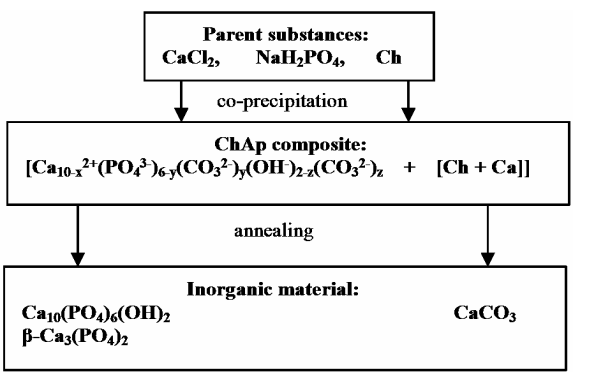

Fig. 6 Proposed scheme of co-precipitation and thermal transformation of ChAp composite. Ch stands for chitosan.

In the IR spectra the bands of carbonate ions of the composites mineral part are present: in the 1600-1400 cm^{-1} region (ν_3 antisymmetric valence vibrations of C-O) and 880-870 cm^{-1} (ν_2 lateral deformation vibrations of C-O-C). This indicates that the apatite contains CO_3 ions, located both in the position of PO_4 anion (type B carbonate substitution: 1455 cm^{-1}, 1410 cm^{-1} and 875 cm^{-1}), and in the OH-channel (type A substitution: 1545 cm^{-1} and 1450 cm^{-1}) [21]. The relative intensity of spectral bands changes when the temperature of a sample increases. This can be explained by the release of carbonates located in the OH-channel: they are getting substituted by hydroxyl ions; at the same time, the carbonate ions, substituting phosphate groups, remain in their positions. The substitution of phosphate ions by carbonate ions in the apatite structure has to be accompanied by the vacancy formation in the cation sublattice (electroneutrality requirement). This is in good agreement with the data of XRD phase analysis showing the thermal decomposition of apatite with β-TCP formation.

From the analysis of the thermal behaviour of carbonate IR spectral bands one can conclude that the carbonate transits from the labile state to the position of apatite phosphate ion. The substitution degree of phosphate ions by carbonate ions increases with the increase of annealing temperature. It can be supposed that the formation and migration of carbonate ions are caused by pyrolytic decomposition of chitosan and thermally activated entrapping of the products of this decomposition by the crystal lattice of the mineral.

When the annealing temperature rises, starting from 700 °C, the intensities of the wide band at 3600-3200 cm^{-1} (associated with symmetric and antisymmetric vibrations of OH-groups in water molecules) and the

band at 1630-1570 cm^{-1} (reflecting the deformation vibrations of H-O-H groups) decrease noticeably. This indicates the significant decrease of water molecules concentration localized presumably in the near-surface layers of HA crystallites. Under annealing at 900 °C the characteristic narrow peak at 3645 cm^{-1} emerges. This peak corresponds to the valence vibrations of hydroxyl ions in the OH-channel of HA [20].

Summarizing the above, a possible scheme of co-precipitation and thermal transformation of ChAp can be suggested (Fig. 6). It is reasonable to suppose that the calcium entrapped by chitosan matrix is more biologically available in comparison with the calcium which belongs to the apatite lattice. If so, the calcium from chitosan matrix can be more easily used for the regenerated bone formation at the initial stages of reparation. This may reduce the need of calcium mobilization from the surrounding living bone tissue as well as from the mineral part of the composite material. The slower utilization of the apatite calcium could prevent undesirable degradation of mechanical characteristics in the implantation site.

4 Conclusion

The data of X-ray diffraction, FTIR spectroscopy and scanning electron microscopy with EDX analysis of the annealed samples of chitosan-apatite composites show that the formation of calcium-phosphate mineral in the chitosan solution is modulated significantly by the chemical interactions of the components; part of calcium is probably entrapped by the chitosan molecules and does not participate in the formation of the main mineral phase. The apatite in the composites is calcium-deficient and carbonate-substituted; it is characterized by nano-sized crystallites. The results suggest the homogeneous and dispersed distribution of randomly oriented apatite nanocrystals in chitosan matrix. Varying the conditions of synthesis, drying and lyophilization it is possible to obtain the chitosan-calcium apatite composites with different components ratios, and in the form of either solid or porous material.

References

[1] I. Yamaguchi, K. Tokuchi, H. Fukuzaki, Y. Koyama, K. Takakuda, H. Monma, and J. Tanaka, J. Biomed. Mater. Res. **55**, 20 (2001).
[2] Y. Zhang and M. Q. Zhang, J. Biomed. Mater. Res. **55**, 304 (2001).
[3] Q. Hu, B. Li, M. Wang, and J. Shen, Biomaterials **25**, 779 (2004).
[4] V. M. Rusu, C.-H. Ng, M. Wilke, B. Tiersch, P. Fratzl, and M. G. Peter, Biomaterials **26**, 5414 (2005).
[5] I. B. Leonor, E. T. Baran, M. Kawashita, R. L. Reis, T. Kokubo, and T. Nakamura, Acta Biomater. **4**, 1349 (2008).
[6] B. M. Chesnutt, A. M. Viano, Y. Yuan, Y. Yang, T. Guda, M. R. Appleford, J. L. Ong, W. O. Haggard, and J. D. Bumgardner, J. Biomed. Mater. Res. A **88**, 491 (2009).
[7] M. J. Glimcher, Bone: Nature of the Calcium Phosphate Crystals and Cellular, Structural, and Physical Chemical Mechanisms in Their Formation. Series: Reviews in mineralogy and geochemistry, Vol. 64 (Mineralogical Society of America, Washington, 2006).
[8] J. C. Elliott, in: Phosphates: geochemical, geobiological and materials importance. Series: Reviews in mineralogy and geochemistry, Vol. 48 (Mineralogical Society of America, Washington, 2002) pp. 427-453.
[9] I. Manjubala, S. Scheler, J. Bössert, and K. D. Jandt, Acta Biomater. **2**, 75 (2006).
[10] J. M. Oliveira, M. T. Rodrigues, S. S. Silva, P. B. Malafaya, M. E. Gomes, C. A. Viegas, I. R. Dias, J. T. Azevedo, J. F. Mano, and R. L. Reis, Biomaterials **27**, 6123 (2006).
[11] J. Liu, F. Shi, L. Yu, L. Niu, and S. Gao, J. Mat, Sci. Technol. **25**, 551 (2009).
[12] A. Bigi, E. Boanini, M. Gazzano, and K. Rubini, Cryst. Res. Technol. **40**, 1094 (2005).
[13] S. N. Danilchenko, A. V. Koropov, I. Yu. Protsenko, B. Sulkio-Cleff, and L. F. Sukhodub, Cryst. Res. Technol. **41**, 263 (2006).
[14] D. L. Bish and J. E. Post, Modern powder diffraction, Reviews in mineralogy, Vol. 20, P. H. Ribbe ed. (Mineralogical Society of America, Washington, 1989).
[15] S. N. Danilchenko, O. G. Kukharenko, C. Moseke, I. Yu. Protsenko, L. F. Sukhodub, and B. Sulkio-Cleff, Cryst. Res. Technol. **37**, 1234 (2002).
[16] S. Pramanik, A. K. Agarwal, and K. N. Rai, Trends Biomater. Artif. Organs. **19**, 46 (2005).
[17] S. N. Danilchenko, I. Yu. Protsenko, and L. F. Sukhodub, Cryst. Res. Technol. **44**, 553 (2009).
[18] S. Raynaud, E. Champion, D. Bernache-Assollant, and J.-P. Laval, J. Am. Ceram. Soc. **84**, 359 (2001).
[19] B. O. Fowler, Inorg. Chem. **13**, 207 (1974).
[20] K. Nakamoto, Infrared and Raman Spectra of Inorganic and Coordination Compounds, (Wiley-Interscience, John Wiley and Sons, New York, 1986).
[21] M. E. Fleet, Biomaterials **30**, 1473 (2009).

